



Semnan University

Mechanics of Advanced Composite Structures

journal homepage: <http://MACS.journals.semnan.ac.ir>

Initial Buckling Behavior of Elastically Supported Rectangular FGM Plate based on Higher Order Shear Deformation Theory via Spline RBF Method

R. Kumar ^{a*}, H. K. Sharma ^b, S. Gupta ^c, A. Malguri ^d, B. Rajak ^e,
Y. Srivastava ^f, S. Khan ^g, A. Pandey ^h

^a Department of Mechanical Engineering DDU, Gorakhpur, India

^b Department of Mechanical Engineering, GLA University, Mathura, India

^c Department of Civil Engineering MMMUT, Gorakhpur, India

^d Oil and gas, HEPIPL, Adani Group, Ahmedabad, India

^e Department of Mechanical Engineering IIT, BHU, India

^f Department of Mechanical Engineering MMMUT, Gorakhpur, India

^g Mechanical Engineering SGI, Kukas, Jaipur, India

^h Department of Mechanical Engineering DDU, Gorakhpur, India

KEYWORDS

FGM plate;
Spline RBF;
Meshfree;
Buckling;
Foundation;
Aspect ratio.

ABSTRACT

In the present paper, the effect of aspect ratio on the initial buckling response of an elastically supported rectangular FGM plate, the thin plate spline radial basis function (RBF) method can be used. This method involves the use of a thin plate spline to interpolate the displacement field of the plate, allowing for accurate analysis of the plate's behavior. The higher-order shear deformation theory (HSDT) is used for the analysis of the FGM rectangular plate resting on two parameters of elastic foundation. The displacement field consists of five unknown variables and approximately parabolic distribution of the transverse stress profile through the plate thickness and tangential stress-free boundary conditions on the plate surface. The governing differential equations (GDEs) of the plate are developed in the framework of Hamilton's principle. The thin plate spline radial basic function-based Meshfree method is used for discretizing the GDEs. To demonstrate the accuracy and efficacy of the present approach, the results obtained by the present approach are compared with the results given in the literature. The effect of various aspect ratios, grading index, span-to-thickness ratio, and two parameters of elastic foundations on the normalized buckling load is proposed. Some new results are also presented, which may be beneficial for future research works. The novelty of the present is the effects of aspect ratio on the elastically supported FGM plates.

1. Introduction

Functionally graded materials (FGMs) are a class of advanced engineering materials that have a continuously varying composition and structure over their volume. The composition and structure of FGMs are designed to change gradually from one end to the other, resulting in a material with unique properties that can be tailored for specific applications. FGMs are typically made by combining two or more materials with different properties, such as metals and ceramics, and then gradually varying the composition of each material along a

specified direction. The resulting material can have a wide range of properties, such as high strength, toughness, and wear resistance, as well as the ability to withstand high temperatures and harsh environments. FGMs have a wide range of applications in various fields, such as aerospace, automotive, biomedical, and energy. For example, FGMs can be used in aircraft engines to improve their thermal and mechanical properties, or in dental implants to promote bone growth and integration with the surrounding tissue.

Various numerical techniques are being widely implemented for buckling analysis of

* Corresponding author. Tel.: +91-7543934007
E-mail address: rahul22mech@gmail.com

FGMs rectangular plates so far by researchers. In this direction, Feldman and Aboudi [1] investigated the analytical technique for the buckling analysis of FGM plates subjected to a uniaxial compression load using classical plate theory (CPT). Mohammadi et al. [2] carried out a Levy solution for the buckling response of thin FGMs rectangular plates via the CPT model. Bodaghi and Saidi [3] studied analytical techniques for the buckling response of thick FGM plates based on HSDT. Thai and Uy [4] carried out analytical solutions for the buckling response of FGMs plate via refined plate theory. Singh and Harsha [5] examined the buckling response of FGM plates subjected to various types of in-plane loads in the framework of the HSDT model. However, these analytical solutions are not pertinent for general cases, and they are not yet feasible for complex geometry and loading conditions. Subsequently, various numerical methods are being utilized, such as the finite elements method (FEM) [6], meshless method, spline finite strip method, and so for. Among various numerical methods, the mesh-free technique has long been utilized as one of the most effective numerical methods for the buckling response of plates. Bateni et al. [7] examined the initial buckling response of FGM plates under thermal and mechanical loading via the Galerkin method. Bui et al. [8] studied the stability response of the plate using the moving Kriging interpolation technique. Liew et al. [9] studied the buckling and vibration response of plates using the reproducing kernel particle approximate technique and first-order shear deformation theory (FSDT). Kiarasi et al., [10] investigated buckling analysis of sandwich plates via analytical approach and classical plate theory. Shahani and Kiarasi, [11] studied the post-buckling response of shells with rectangular cutouts under axial loading via the finite element method (FEM). Kumari et al. [12] carried out a stress analysis of a single hole on an infinite plate via Airy's stress function. Rahul and Singh [13] examined the buckling analysis of the FGM plate via the RBF technique. Tan et al. [14] investigated 3D isogeometric analysis and mesh-free coupling approach to examine the structural responses for FGM structures. Kiarasi et al. [15] investigated the buckling response of porous FGM rectangular plates subjected to different loading conditions. Asemi et al. [16] developed a 3D FEM formulation for the buckling response of anisotropic FGMs plate with arbitrary orthotropy directions. Shahsavari et al. [17] investigated thermal post-buckling analysis of FGM annular sector plates subjected to uniform temperature rise via FEM approach. Singh et al. [18] used the molecular dynamics approach for the mechanical properties of multi-walled carbon nanotubes.

Khatoonabadi et al., [19] studied shear buckling analysis of FGM annular sector plate reinforced with graphene nanoplatelets (GPLs) under porous medium via FEM approach. Kumar et al. [20] studied the wear response of FGM under the influences of centrifugal casting processing. Neves et al. [21] examined the structural response of sandwich plates via quasi-3D HSDT and mesh-free methods. Singh et al. [18] investigated the effect of functionalization on the mechanical properties of multi-walled carbon nanotubes. Rahimi et al. [22] studied the exact thermoelastic response of an FGM piezoelectrical rotating cylinder with the combination of electrical, thermal, and mechanical loads simultaneously. Arefi and Rahimi [23] studied the 2D electro-elastic response of an FGM piezoelectric cylinder under internal pressure using the FSDT model. Arefi and Rahimi [24] investigated different boundary conditions for the thermoelastic response of an FG cylinder via the FSDT model. Arefi and Zenkour [25] studied the nonlocal thermo-magneto-electro-mechanical bending response of a three-layered nanoplate via sinusoidal shear-deformation plate theory. Ferreira et al. [26] studied the buckling and vibration analysis of laminated plates via the RBF technique and FSDT model. Rodrigues et al. [27] applied Murakami's zig-zag theory with RBF- finite difference collocation method for the structural analysis of composite plate. Rahimi et al. [28] examined the electro-elastic response of FGM piezoelectric cylinder via FSDT model. Khoshgoftar et al. [29] examined the elastic response of a FGM thick-walled cylindrical via FSDT model and analytical approach. Arefi and Rahimi [30] investigated nonlinear analysis of a FG square plate with two smart layers as a sensor and actuator under pressure using Von-Karman assumption. Ferreira et al. [31] investigated the stability response of isotropic and laminated plates via the FSDT model and RBF with wavelets. Chilakala et al. [32] used Element Free Galerkin Method for the Cracks analysis in Automotive Coatings Under Mechanical and Thermal Loading. Kumar et al. [33] investigated the thermomechanical buckling response of a bi-directional porous FGM plate using HSDT displacement field. Arefi and Rahimi [34] studied the nonlinear response of the FGM piezoelectric annular plate in the framework of Von-Karman assumption. Arefi and Rahimi [35] introduced the 3D multi-field formulation of a FGM piezoelectric thick shell of revolution via tensor analysis

To represent the correlation between the plate and foundation, different types of foundation models have been considered so far. The plate supported by the elastic foundation is increasingly used in many structural applications such as the foundation of runways of large

aircraft, foundation deep wells, bridges and buildings, etc. The easiest one is the Winkler model, which considers the establishment as a progression of isolated springs without coupling impacts among one another [36]. Pasternak alters this model by considering a shear spring among the isolated springs in Winkler's model, known as the two-parameters model [37]. Thai et al. [38] examined the structural response of elastically supported plates using a simple, refined theory. Malekzadeh and Karami [39] applied mixed differential quadrature and FEM for vibration and stability response of elastically supported thick beams.

Sobhy [40] examined the stability and vibration analysis of elastically supported FGM sandwich plates. In the above-mentioned literature, little work has been done for buckling analysis of thin and thick rectangular FGM plates supported by the elastic foundation to the best of the author's knowledge. Modified thin plate spline RBF-based mesh-free method capable of producing a result for rectangles without changing the shape parameter.

In the present work, the influence of the aspect ratio of an elastically supported rectangular FGM plate is carried out for the initial buckling response. The displacement field is based on five variables HSDT model. The governing differential equations and boundary conditions are derived using Hamilton's principle. The thin plate spline RBF-based Meshfree method is implemented for discretizing the GDE. The accuracy of the present code is verified by convergence study and the results obtained by the present method are compared with reported results available in the literature. The aspect ratio of a structure significantly affects its buckling behavior. Design considerations for buckling stability should take into account the aspect ratio to ensure the structural integrity and safety of the system. The influences of grading index, foundation parameters, span-to-thickness ratio, and plate aspect ratio on the initial buckling of rectangular FGMs are discussed.

2. Mathematical Formulation

A FGM plate with dimensions a , b , and h indicated as length, width, and thickness, respectively, in the coordinates x - y and z -axis are shown in Fig. 1. The reference plane is considered from the mid-plane of the plate.

The volume fraction of the metal side is expressed as [41]

$$V_m(z) = 1 - V_c(z) \tag{1}$$

where n is the volume fraction of metal. The material property (Young's modulus, E where

subscripts m and c represent the metallic and ceramic) varying through the thickness of the plate is expressed as [42],[43],[44]

$$E(z) = [E_c - E_m] V_c(z) + E_m \tag{2}$$

where $V_c(z) = \left(\frac{2z+h}{2h}\right)^n$

The effect of variation of Poisson's ratio (ν) is assumed as constant.

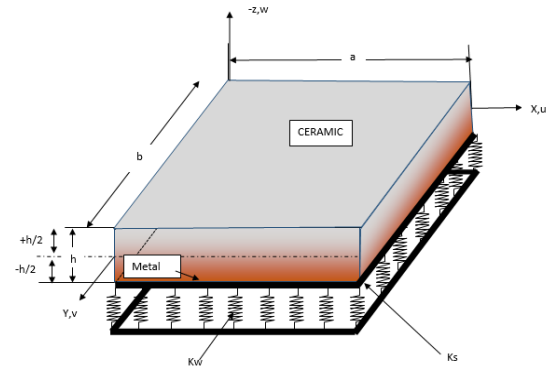


Fig. 1. The elastically supported FGM plate

The relationship between the FGM plate and supporting foundation is expressed as [45],[46]

$$k_w w - k_s \left(\frac{\partial^2 w}{\partial x^2} + \frac{\partial^2 w}{\partial y^2} \right)^2 \tag{3}$$

where the parameters k_w and k_s are the normal and shear stiffness of the foundation, respectively.

2.1. Displacement Field

Assuming the displacement components u and v are the inplane displacements in the x and y directions respectively and w is the transverse displacement in the z -direction. These displacements are small in comparison with the plate thickness. The in-plane displacement u in the x -direction and v in the y -direction each consist of two parts: (a) a displacement component analogous to displacement in classical plate theory of bending; (b) a displacement component due to shear deformation which is assumed to be parabolic in nature with respect to thickness coordinate. The present displacement field is assumed to be the HSDT model with five unknown displacement variables expressed as [47]:

$$\begin{aligned} u &= u_0(x, y) - z \frac{\partial w_0(x, y)}{\partial x} + f(z) \phi_x(x, y) \\ v &= v_0(x, y) - z \frac{\partial w_0(x, y)}{\partial y} + f(z) \phi_y(x, y) \\ w &= w_0(x, y) \end{aligned} \tag{4}$$

where, $f(z) = p \left(\left(\frac{z}{h} \right)^3 - \frac{3}{4h} z \right)$ is a transverse shear function where $p=0.9$

2.2. Stress-Strain Relations

The Generalise Hook's law for the isotropic FGM plate is represented as [48];

$$\begin{Bmatrix} \sigma_{xx} \\ \sigma_{yy} \\ \sigma_{xy} \\ \sigma_{yz} \\ \sigma_{zx} \end{Bmatrix} = \begin{bmatrix} \bar{Q}_{11} & \bar{Q}_{12} & 0 & 0 & 0 \\ \bar{Q}_{12} & \bar{Q}_{22} & 0 & 0 & 0 \\ 0 & 0 & \bar{Q}_{66} & 0 & 0 \\ 0 & 0 & 0 & \bar{Q}_{44} & 0 \\ 0 & 0 & 0 & 0 & \bar{Q}_{55} \end{bmatrix} \begin{Bmatrix} \varepsilon_{xx} \\ \varepsilon_{yy} \\ \gamma_{xy} \\ \gamma_{yz} \\ \gamma_{zx} \end{Bmatrix} \quad (5)$$

2.3. Governing Differential Equations

The GDEs of the elastically supported FGM plate are produced by the energy principle and collecting the coefficients of variables $\delta u_0, \delta v_0, \delta w_0, \delta \phi_x$ and $\delta \phi_y$, as [49], [54],[55].

$$\delta u_0 : \frac{\partial N_{xx}}{\partial x} + \frac{\partial N_{xy}}{\partial y} = 0 \quad (6)$$

$$\delta v_0 : \frac{\partial N_{xy}}{\partial x} + \frac{\partial N_{yy}}{\partial y} = 0 \quad (7)$$

$$\begin{aligned} \delta w_0 : & \frac{\partial^2 M_{xx}}{\partial x^2} + \frac{\partial^2 M_{yy}}{\partial y^2} + 2 \frac{\partial^2 M_{xy}}{\partial x \partial y} \\ & + k_w w_0 - k_s \left(\frac{\partial^2 w_0}{\partial x^2} + \frac{\partial^2 w_0}{\partial y^2} \right) \\ & = N_{xx}^b \frac{\partial^2 w}{\partial x^2} + N_{yy}^b \frac{\partial^2 w}{\partial y^2} \end{aligned} \quad (8)$$

$$\delta \phi_x : \frac{\partial M_{xx}^f}{\partial x} + \frac{\partial M_{xy}^f}{\partial y} - Q_x^f = 0 \quad (9)$$

$$\delta \phi_y : \frac{\partial M_{xy}^f}{\partial x} + \frac{\partial M_{yy}^f}{\partial y} - Q_y^f = 0 \quad (10)$$

where, N_{xx}^b and N_{yy}^b are the in-plane axial forces along x and y directions, respectively. Uniaxial compression along the x-axis is $N_{xx}^b = 1, N_{yy}^b = 0$ known as Uniaxial -A type and uniaxial compression along the y-direction $N_{xx}^b = 0, N_{yy}^b = 1$ is known as Uniaxial-B type and the rest is biaxial compression along the x- and y-axes as $N_{xx}^b = 1, N_{yy}^b = 1$ shown in Fig. 2.

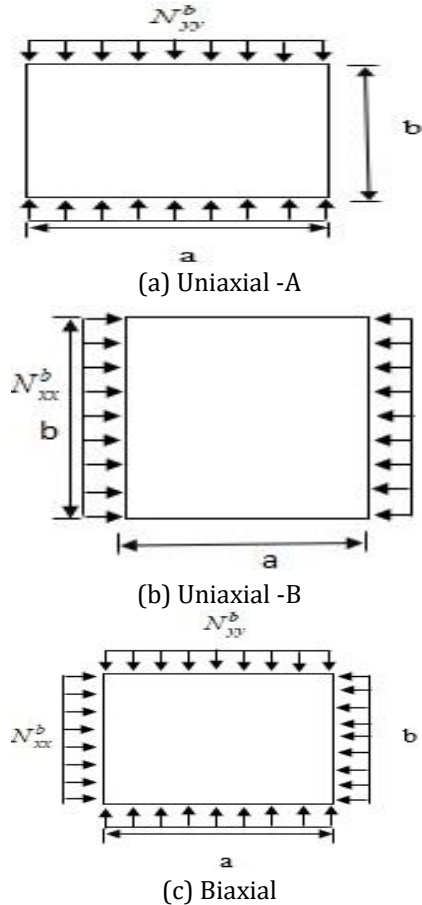


Fig. 2. Types of in-plane forces of FGM rectangular plates

The boundary condition for simply supported plate is expressed as [25-26]

$$\begin{aligned} x = 0, a : & N_{xx} = 0, v_0 = 0, w_0 = 0, M_{xx} = 0, \phi_y = 0 \\ y = 0, b : & u_0 = 0, N_{yy} = 0, w_0 = 0, \phi_x = 0, M_{yy} = 0 \end{aligned} \quad (11)$$

3. The Numerical Implementation

The RBF is a mathematical function that depends only on the distance between the input points and some fixed center points in a multidimensional space. In other words, the value of an RBF at any point in the space is determined by the distance between that point and a set of predefined center points. However, the method's accuracy and stability are extremely dependent on an appropriate choice of a shape parameter 'c'. The solution of the linear GDEs is assumed in terms of modified thin plate spline RBF $g(\|X - X_j\|, c)$ expressed as for nodes 1: N, as;

$$\log \left(\sqrt{\left(\frac{x-x_j}{a} \right)^2 + \left(\frac{y-y_j}{b} \right)^2} \right) \cdot \left(\sqrt{\left(\frac{x-x_j}{a} \right)^2 + \left(\frac{y-y_j}{b} \right)^2} \right)^{2c}$$

where a and b are the length and breadth of the rectangular plate and 'c' is the shape parameter. First, the convergence of results is checked by shifting the shape parameter. When convergence

is achieved within 1% and is stable, the accuracy is verified. The unknown field variables u_0, v_0, w_0, ϕ_x and ϕ_y appearing in governing differential equations are assumed in terms of radial basis function as [51],[52],[53]:

$$u_0(x, y) = \sum_{j=1}^N \alpha_j^{u_0} g(\|X - X_j\|, c) \tag{12}$$

$$v_0(x, y) = \sum_{j=1}^N \alpha_j^{v_0} g(\|X - X_j\|, c) \tag{13}$$

$$w_0(x, y) = \sum_{j=1}^N \alpha_j^{w_0} g(\|X - X_j\|, c) \tag{14}$$

$$\phi_x(x, y) = \sum_{j=1}^N \alpha_j^{\phi_x} g(\|X - X_j\|, c) \tag{15}$$

$$\phi_y(x, y) = \sum_{j=1}^N \alpha_j^{\phi_y} g(\|X - X_j\|, c) \tag{16}$$

where, N is the total number of nodes, which is equal to the summation of boundary nodes NB and domain interior nodes NI, α_j^u is an unknown coefficient, $g(\|X - X_j\|, c)$ is radial basis function, $\|X - X_j\|$ is the distance between the nodes and c is the shape parameter.

The discretized GDEs for buckling analysis are written as:

$$\left[\begin{matrix} [K]_L + [K]_{I,F} \\ [K]_B + [K]_{B,F} \end{matrix} \right]_{N \times N} + \lambda \begin{bmatrix} [K]_G \\ 0 \end{bmatrix}_{N \times N} \{ \delta \}_{N \times 1} = 0 \tag{17}$$

$$[K]_I = \begin{bmatrix} [K^I_{1u}]_{(NI,N)} & [K^I_{1v}]_{(NI,N)} & [K^I_{1w}]_{(NI,N)} & [K^I_{1\phi_x}]_{(NI,N)} & [K^I_{1\phi_y}]_{(NI,N)} \\ [K^I_{2u}]_{(NI,N)} & [K^I_{2v}]_{(NI,N)} & [K^I_{2w}]_{(NI,N)} & [K^I_{2\phi_x}]_{(NI,N)} & [K^I_{2\phi_y}]_{(NI,N)} \\ [K^I_{3u}]_{(NI,N)} & [K^I_{3v}]_{(NI,N)} & [K^I_{3w}]_{(NI,N)} & [K^I_{3\phi_x}]_{(NI,N)} & [K^I_{3\phi_y}]_{(NI,N)} \\ [K^I_{4u}]_{(NI,N)} & [K^I_{4v}]_{(NI,N)} & [K^I_{4w}]_{(NI,N)} & [K^I_{4\phi_x}]_{(NI,N)} & [K^I_{4\phi_y}]_{(NI,N)} \\ [K^I_{5u}]_{(NI,N)} & [K^I_{5v}]_{(NI,N)} & [K^I_{5w}]_{(NI,N)} & [K^I_{5\phi_x}]_{(NI,N)} & [K^I_{5\phi_y}]_{(NI,N)} \end{bmatrix}_{(5NI \times 5N)} \tag{18}$$

$$[K]_G = \begin{bmatrix} [0] & [0] & [0] & [0] & [0] \\ [0] & [0] & [0] & [0] & [0] \\ [0] & [0] & [G^I_{3w_0}] & [0] & [0] \\ [0] & [0] & [0] & [0] & [0] \\ [0] & [0] & [0] & [0] & [0] \end{bmatrix}_{(5 \times NI, 5 \times N)} \tag{19}$$

$$[K]_{I,F} = \begin{bmatrix} [0] & [0] & [0] & [0] & [0] \\ [0] & [0] & [0] & [0] & [0] \\ [0] & [0] & [K_w w_0 - K_s \left(\frac{\partial^2 w_0}{\partial x^2} + \frac{\partial^2 w_0}{\partial y^2} \right)] & [0] & [0] \\ [0] & [0] & [0] & [0] & [0] \\ [0] & [0] & [0] & [0] & [0] \end{bmatrix}_{(5 \times NI, 5 \times N)} \tag{20}$$

$$[K]_{B,F} = [0]_{(5 \times NB, 5 \times N)} \tag{21}$$

The final matrix in the form of unknown variables is written as above. For calculating the unknown variables, a generalized MATLAB code is developed as it is easy for matrix operations to find out the unknown variables.

4. Results and Declaration

Several numerical examples are presented for buckling analysis of FGM rectangular plates with different plate aspect ratios and thickness ratios for uniaxial and biaxial compressions, along with varying parameters of foundation. FGM plate is assumed as simply supported, and the material properties used in computations are as $E_c=360$ GPa, $E_m=70$ GPa, and $\nu=0.3$.

The following non-dimensional critical buckling (\bar{N}_{cr}) is expressed as $\bar{N}_{cr} = N_{cr} a^2 / E_m h^3$ where N_{cr} is the critical dimensional buckling load.

The Winkler (K_w) and shear foundation parameters (K_s) are expressed as

$$K_s = \frac{ks12(1-\nu^2)}{Emh^3} \quad \text{and} \quad K_w = \frac{kw12(1-\nu^2)}{Emh^3}$$

where K_s and K_w are the input shear and spring foundation parameters.

4.1. Convergence and Validation

The convergence and comparison study for the normalized buckling with respect to the number of nodes is presented in Table 1 for $a/h=10$, $a/b=0.5$, and $k_s=0$, $k_w=0$. The present results are compared with results available in literature by Kulkarni et al. [56] using the 2D analytical solution based on HSDT and Sekkal et al. [57] using quasi-3D HSDT. It is noted that the present results are in perfect agreement with the results available in the literature, and they converged within 1% and became closer to the results of Kulkarni et al. [56] and Sekkal et al. [57] at 15X 15. It is clearly observed that the present result produced in 15X15 nodes showed 0.04 %

average difference the results of Kulkarni et al. [56] and 2.40 % average difference the results of Sekkal et al. [57] under Uniaxial-B loading and 0.04 % average difference the results of Kulkarni et al. [56] and 2.40 % average difference the results of Sekkal et al. [57] under Biaxial loading Hence 15X15 nodes are taken for further analysis of the numerical study. With the increase of power index law, the dimensionless buckling load decreases due to more content of metal portion being added. In between the uniaxial and biaxial loading, biaxial loading provides better lower buckling resistance as compared to uniaxial loading due to a higher amount of in-plane loading.

4.2. Parametric study

In this section, the influence of aspect ratio on the critical buckling loads of FGM rectangular plate with different span-to-thickness ratios for $a/h = 5, 10$ and 20 under Uniaxial-A load and $n=1$, and $k_s=0, k_w=0$ is investigated and shown in Fig. 3. For the graph with thickness ratio $a/h=5$, it is noticed that by increasing the aspect ratio (a/b) from 0.5 to 0.8, the buckling load start decreases and further increases from 0.9 to 1.2. A similar nature is observed in aspect ratios from 1.3 to 2.3. In addition, with an increase in aspect ratio, the peak of normalized buckling shifted toward the right for all span-to-thickness ratios. The same nature is followed by all the span-to-thickness ratios. For the given aspect ratio, the buckling load increases with the increase of span span-to-thickness ratio.

The influences of aspect ratio with grading index on normalized critical buckling of rectangular FGM plate under uniaxial-A loading is investigated for $a/h=10$, and $K_s=0, K_w=0$ and shown in Fig. 4. It is interesting that with the increase of the gradation index, the buckling load decreases. For the same gradation index, with the increase of aspect ratio, the buckling load decreases from 0.5 to 0.8 and then increases from 0.9 to 1.2, as discussed in the previous example of 2.1.1. For the gradation index $n=0$, the buckling load is highest due to the addition of a fully ceramic portion in the plate.

Further, the effect of aspect ratio on normalized critical buckling of rectangular FGM plate under various loading conditions for $a/h=10, n=2, K_s=0, K_w=0$ is shown in Fig. 5. In addition to the above discussion, it is worth noting that the nature of changing the critical buckling is repeated for Uniaxial-A loading, as discussed in section 4.2.2. For uniaxial-B and biaxial loading, buckling load decreases continuously with the increase of aspect ratio.

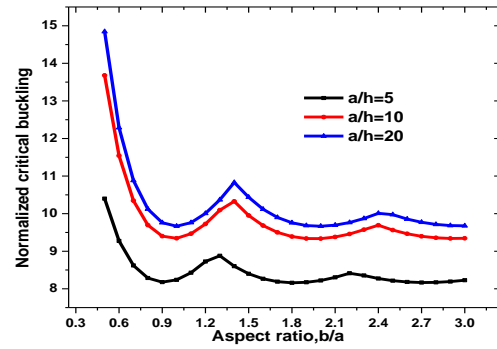


Fig. 3. Effect of plate length to thickness ratio and aspect ratio on normalized critical buckling under Uniaxial-A loading.

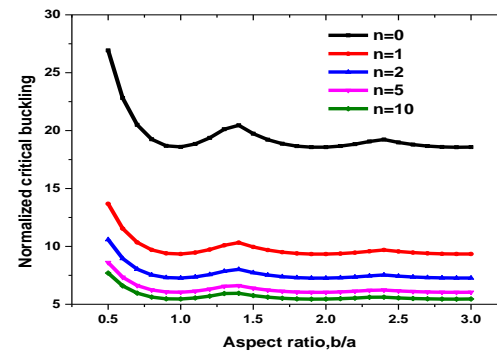


Fig. 4. Effect of aspect ratio and grading index under Uniaxial-A load.

Table 2 represents the contour shape of different aspect ratios ($b/a=0.5, 1, 2$, and 3) on normalized buckling of FGM rectangular plate under Uniaxial-A, Uniaxial-B, and biaxial loading for $a/h=10, n=1$, and $K_s=0, K_w=0$. It is very interesting that the first mode is observed for a small change in aspect ratios (b/a) from 0.5 and 1.0 for uniaxial-A, while the second and third mode is observed for further increase of aspect ratio from 2.0 to onward. For uniaxial-B, the second and first mode is observed for aspect ratio 0.5 and 1.0, and the first mode is observed for further increasing the aspect ratio from 1 to 3. For bi-axial loading, with the increase of aspect ratio, the first mode is observed so far. The reason for changing the shape contour is due to local deformation in the shape of the structure, and more than one apex may be created for the given specific arrangement of uni-axial compression. Among the given different arrangements of Uniaxial-A and Uniaxial-B and bi-axial in-plane loading, with the increase of aspect ratio, buckling load of Uniaxial-A arrangement decreases very sharply from 0.1 to 1 and then very little change is observed for further increase the aspect ratio from 1 to onward. For the Uniaxial-B arrangement, with the increase of aspect ratio, the buckling load decreases very sharply, and a similar trend is observed in bi-axial compression also.

Table 1. Convergence and validation study of FGM rectangular plate under uniaxial-B and biaxial loading.

Loading	Methods	Grading Index						Avg.% 2D [51]	Avg. % 3D[52]
		0	0.5	1	2	5	10		
Uniaxial-B	9X9	8.9862	5.364	3.7543	2.6877	2.3787	2.3974	8.59	9.32
	11X11	7.4907	4.8546	3.7215	2.8874	2.4262	2.2127	0.59	2.19
	13X13	7.4187	4.8254	3.7123	2.889	2.4182	2.1938	0.09	2.35
	15X15	7.4079	4.8213	3.711	2.8892	2.4168	2.1906	0.04	2.40
	2D [51]	7.4102	4.8234	3.7131	2.8907	2.4152	2.1904	-----	-----
	3D[52]	7.4126	4.8904	3.8221	3.0168	2.509	2.2374	-----	-----
Biaxial	9X9	7.6392	4.441	3.0673	2.1808	1.9386	1.9807	11.05	11.06
	11X11	5.9935	3.8852	2.9792	2.3121	1.9427	1.7713	0.62	2.13
	13X13	5.9349	3.8604	2.97	2.3115	1.9348	1.7551	0.09	2.34
	15X15	5.9263	3.857	2.9688	2.3114	1.9334	1.7525	0.04	2.40
	2D [51]	5.9281	3.8587	2.9705	2.3125	1.9322	1.7523	-----	-----
	3D[52]	5.9301	3.9123	3.0577	2.4134	2.0072	1.7899	-----	-----

Table 2. Contour shapes of normalized critical buckling for different aspect ratios under various in-plane loadings.

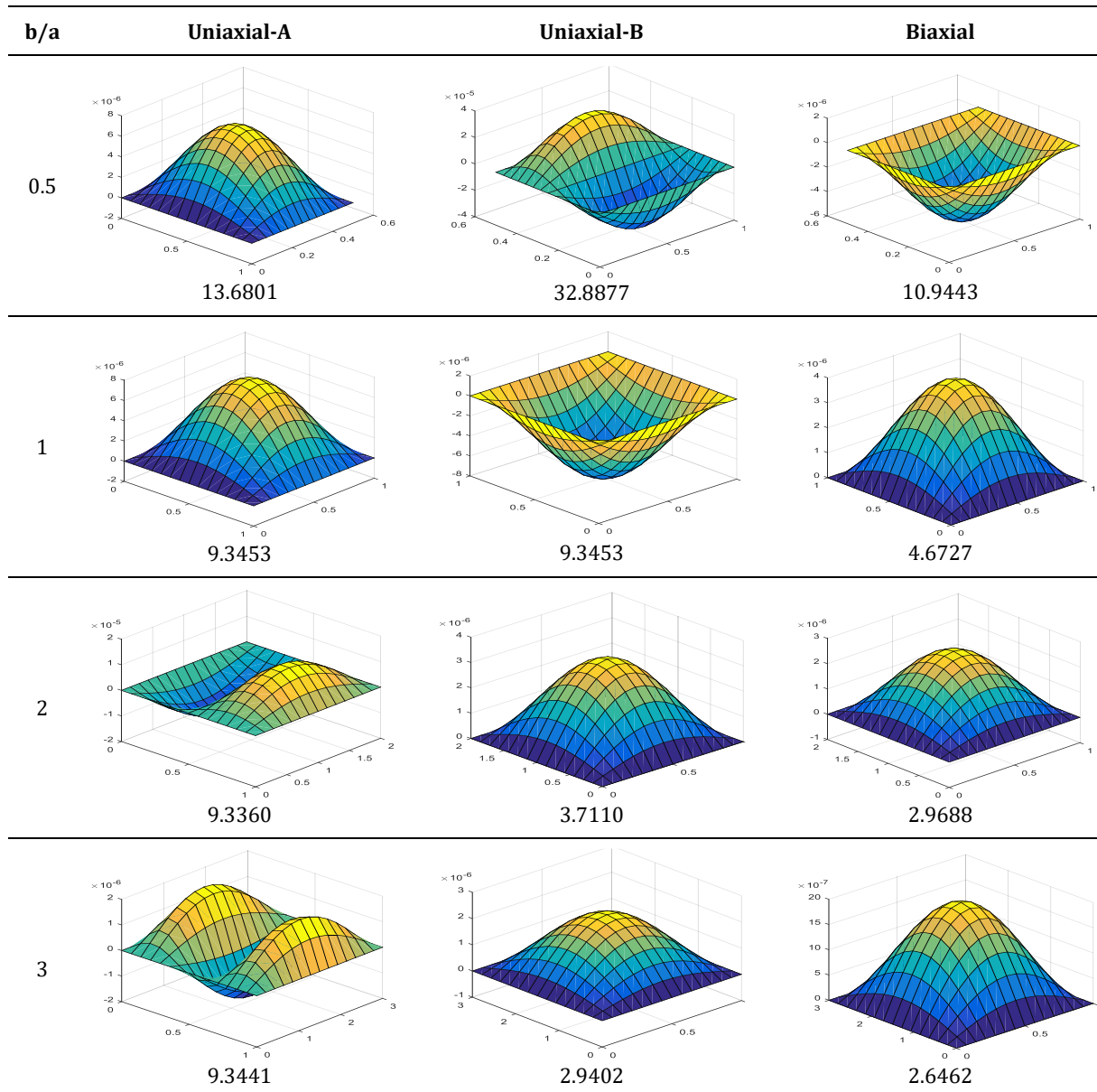


Table 3. Contour shape with the effect of foundation on normalized buckling loads of rectangular FGM plate under in-plane loading.

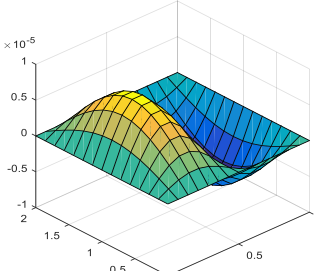
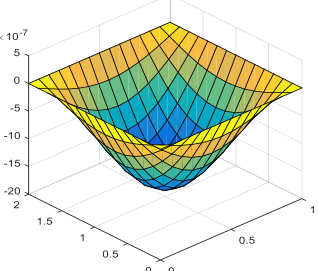
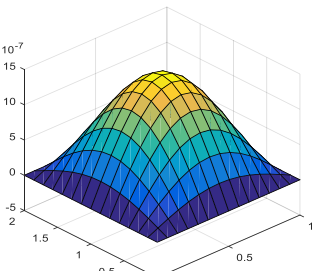
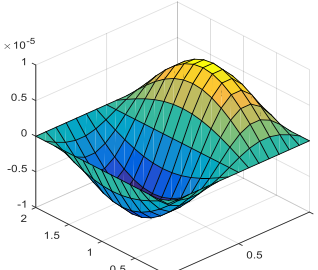
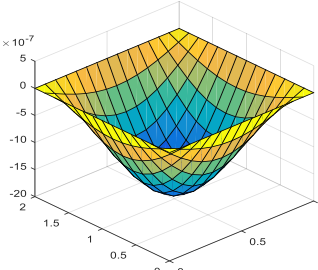
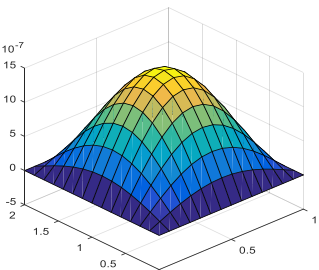
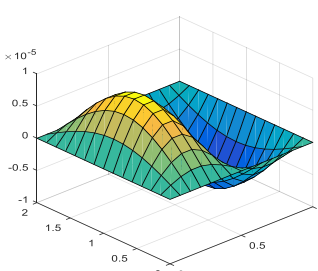
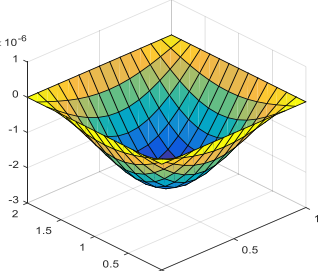
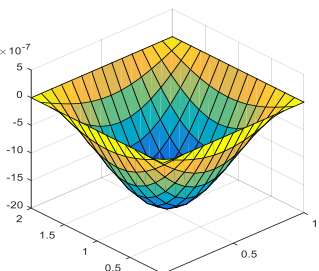
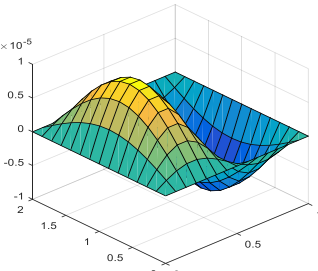
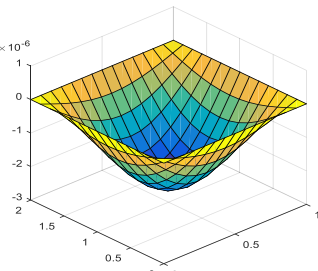
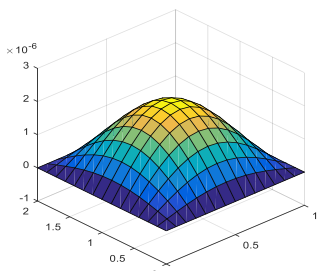
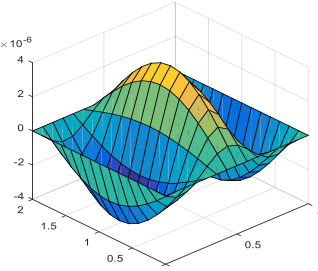
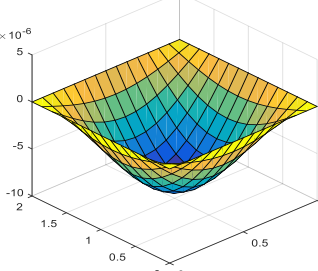
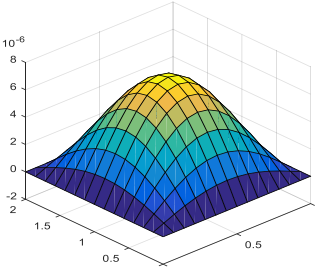
Kw	Ks	Uniaxial -A	Uniaxial -B	Biaxial
0	0	 <p>7.5353</p>	 <p>2.9558</p>	 <p>2.3647</p>
10	0	 <p>7.6281</p>	 <p>3.0485</p>	 <p>2.4389</p>
100	0	 <p>8.4634</p>	 <p>3.8832</p>	 <p>3.1066</p>
0	10	 <p>9.3670</p>	 <p>4.1004</p>	 <p>3.2804</p>
0	100	 <p>22.0088</p>	 <p>14.4024</p>	 <p>11.5222</p>

Table 4. Contour shape of two modes on normalized buckling of FGM plate under uniaxial loading. ($n=2, a/h=20$).

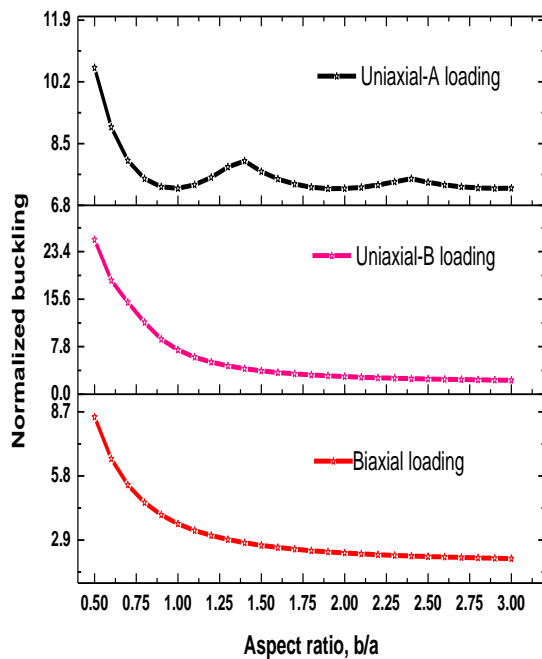
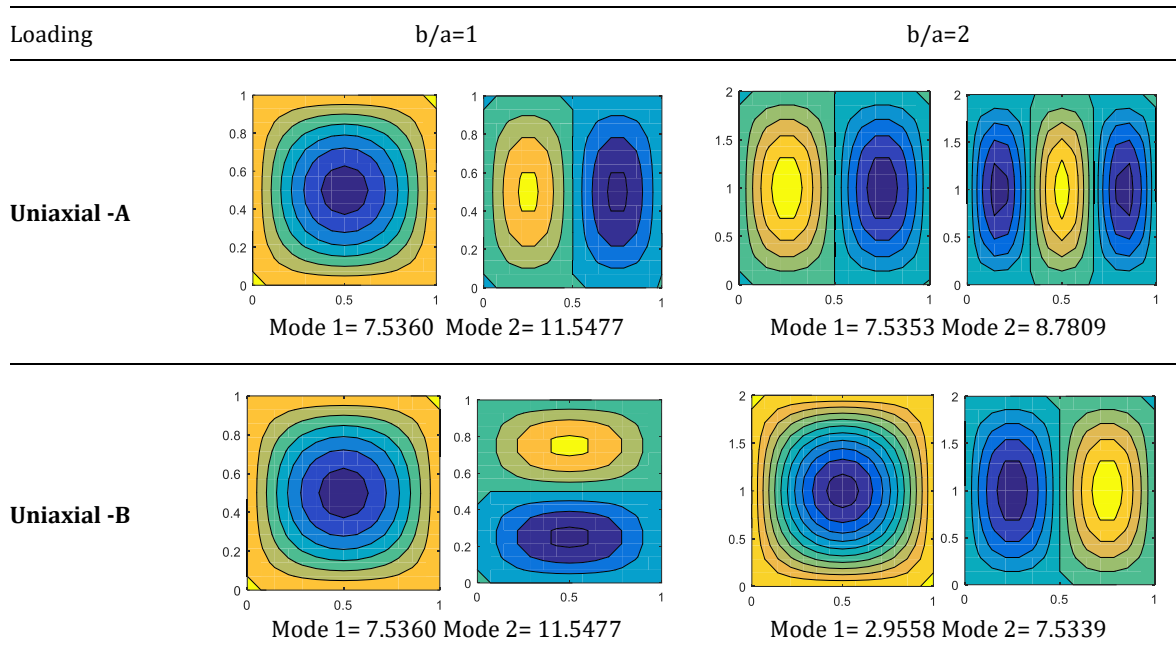


Fig. 5. Effect of aspect ratio under various in-plane loading

The effect of foundation parameters (K_w and K_s) with plate aspect ratios on normalized buckling loads of FGM plate under Uniaxial-B loading is shown in **Fig. 6**. It is observed that at a constant aspect ratio, buckling load increases by increasing Winkler and Pasternak stiffness foundation. This is because the foundation stiffness increases the overall stiffness of the plate. The effect of the Pasternak stiffness foundation is more sensitive than the Winkler

stiffness foundation. It is also observed that the nature followed is similar to the impact of plate aspect ratio in section 4.2.1. It is interesting that for the higher value of shear foundation parameters, the peak of normalized critical buckling is shifted toward the left due to becoming more stronger plate by the action of the foundation.

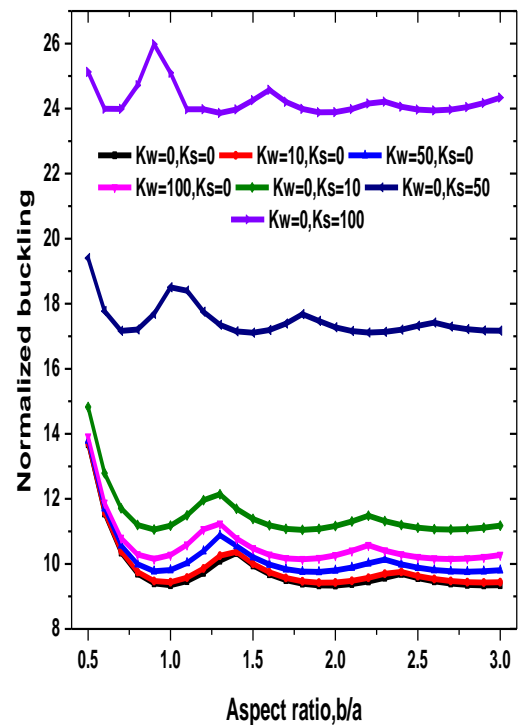


Fig. 6. Effect of elastic foundation with aspect ratios on normalized buckling loads under Uniaxial-B loading. ($a/h=10, n=1$)

The effect of foundation parameters with contour shape on normalized buckling loads of FGM plate under different in-plane loading for $a/h=20$, $n=2$, and $b/a=2$ shown in **Table 3**. It is observed that with the increase of foundation parameters, normalized critical buckling increases due to an increase in the stiffness matrix. The effect of foundation parameters is more severe in Uniaxial-A type arrangement due to higher length along width direction as compared to other Uniaxial-B and biaxial compression. Due to the higher length along the width direction, there would be more than one peak, as shown in the first column of the given Table. It is discussed earlier; the effect of the shear foundation parameter is more crucial on critical buckling load as compared to the Winkler foundation parameter.

Table 4 shows the first two modes shape of a rectangular FGM plate for $a/h=20$, $n=2$, and $b/a=1$ and 2 for uniaxial-A and uniaxial-B loading. In between the two loading conditions, with the increase of aspect ratio, there would be more than one peak in uniaxial-A types of arrangement while there would not be any change in uniaxial-B types of arrangement due to the load acting along x-direction with constant length.

5. Conclusions

In this study, initial buckling analysis of elastically supported rectangular FGM plate using a modified RBF-based meshfree method for different in-plan loading is carried out. The result produced by modified RBF for rectangular plates is in good agreement with the published results. The displacement field with five unknown variables is based on higher-order shear deformation theory. The need for shear correction factor is not required. The GDEs are obtained by deriving the energy principle. The following conclusions are noted from the limited study:

- The normalized critical buckling decreases with the increase of plate aspect ratios in all types of in-plane arrangements, and the Uniaxial-A arrangement would provide higher critical buckling due to the increment of length along the width direction.
- With the increase of thickness ratio, critical buckling load increases due to its dimensionless parameters. However, the dimensional critical buckling load decreases due to the plate becoming thinner.

- In the different arrangements of in-plane loading, The uniaxial-A provides more than one peak for the first buckling mode due to increased width.
- With the increase in the gradation index, normalized critical buckling decreases due to more amount of metal portion added in the FGM.
- Critical buckling of the plate increases when the foundation is attached to the plate due to an increment in the overall stiffness of the plate. The effect of the shear foundation is more severe than the spring foundation due to acting in both the x and y directions.
- The effect of shear foundation in the Uniaxial-A arrangement is more severe for higher values of plate aspect ratios.

Overall, FGMs offer a unique and versatile approach to material design and have the potential to revolutionize many industries in the future. Buckling analysis of these plates can help in optimizing their design and improving their performance under different loading and support conditions. This can ensure the structural integrity and safety of the engineering structures.

Conflicts of Interest

The author declares that there is no conflict of interest regarding the publication of this manuscript.

References

- [1] Feldman, E. and Aboudi, J., 1997. Buckling analysis of functionally graded plates subjected to uniaxial loading, *Composite Structures*, 38, pp. 29–36.
- [2] Mohammadi, M., Saidi, AR., and Jomehzadeh, E., 2010. Levy Solution for Buckling Analysis of Functionally Graded Rectangular Plates, *Appl Compos Mater*, 17, pp. 81–93.
- [3] Bodaghi, M. and Saidi, AR., 2010. Levy-type solution for buckling analysis of thick functionally graded rectangular plates based on the higher-order shear deformation plate theory. *Applied Mathematical Modelling*, 34, pp. 3659–73.

- [4] Thai, H-T. and Uy, B., 2013. Levy solution for buckling analysis of functionally graded plates based on a refined plate theory: *Proceedings of the Institution of Mechanical Engineers, Part C: Journal of Mechanical Engineering Science*, 227, pp. 2649-2664
- [5] Singh, SJ., Harsha, SP., 2019. Buckling analysis of FGM plates under uniform, linear and non-linear in-plane loading. *J Mech Sci Technol*, 33, pp.1761-7.
- [6] Kant, T. and Pandya, BN., 1988. A simple finite element formulation of a higher-order theory for unsymmetrically laminated composite plates. *Composite Structures*, 9, pp.215-46.
- [7] Bateni, M., Kiani, Y. and Eslami, MR., 2013. A comprehensive study on stability of FGM plates. *International Journal of Mechanical Sciences*, 75, pp.134-44.
- [8] Bui, T.Q., Naguyen, M.N. and Zhang, Ch., 2011. Buckling analysis of Reissner-Mindlin plates subjected to in-plane edge loads using a shear-locking-free and meshfree method. *Engineering Analysis with Boundary Elements*, 35, pp. 1038-53.
- [9] Liew, KM., Wang, J., Ng, TY. and Tan, MJ., 2004. Free vibration and buckling analyses of shear-deformable plates based on FSDT meshfree method. *Journal of Sound and Vibration*, 276, pp.997-1017.
- [10] Kiarasi, F., Babaei, M., Dimitri, R. and Tornabene, F., 2021. Hygrothermal modeling of the buckling behavior of sandwich plates with nanocomposite face sheets resting on a Pasternak foundation. *Continuum Mech Thermodyn*, 33, pp.911-32.
- [11] Shahani, AR. and Kiarasi, F., 2023. Numerical and Experimental Investigation on Post-buckling Behavior of Stiffened Cylindrical Shells with Cutout subject to Uniform Axial Compression. *Journal of Applied and Computational Mechanics*, 9, pp.25-44.
- [12] Kumari, S., Pardeep and Bandhu, D., 2022. Stress analysis of an infinite plate with single hole by using Airy's stress function. *Materials Today: Proceedings*, 62, pp.3289-94.
- [13] Kumar, R. and Singh, J., 2018. Assessment of higher order transverse shear deformation theories for modeling and buckling analysis of FGM plates using RBF based meshless approach. *Multi Modelg in Mat & Struct*.
- [14] Tan, P., Nguyen-Thanh, N., Rabczuk, T. and Zhou, K., 2018. Static, dynamic and buckling analyses of 3D FGM plates and shells via an isogeometric-meshfree coupling approach. *Composite Structures*, 198, pp.35-50.
- [15] Kiarasi, F., Babaei, M., Asemi, K., Dimitri, R. and Tornabene, F., 2021. Three-Dimensional Buckling Analysis of Functionally Graded Saturated Porous Rectangular Plates under Combined Loading Conditions. *Applied Sciences*, 11, pp. 10434.
- [16] Asemi, K., Shariyat, M., Salehi, M. and Ashrafi, H., 2013. A full compatible three-dimensional elasticity element for buckling analysis of FGM rectangular plates subjected to various combinations of biaxial normal and shear loads. *Finite Elements in Analysis and Design*, 74, pp.9-21.
- [17] Shahsavari, M., Asemi, K., Babaei, M. and Kiarasi, F., 2021. Numerical Investigation on Thermal Post-buckling Of Annular Sector Plates Made of FGM Via 3D Finite Element Method. 8, pp. 309-20.
- [18] Singh, PK., Sharma, K., Kumar, A., Shukla, M., 2017. Effects of functionalization on the mechanical properties of multiwalled carbon nanotubes: A molecular dynamics approach. *Journal of Composite Materials*, 51, pp. 671-80.
- [19] Khatoonabadi, M., Jafari, M., Kiarasi, F., Hosseini, M., Babaei, M., Asemi, K., 2023. Shear buckling response of FG porous annular sector plate reinforced by graphene platelet subjected to different shear loads. *Journal of Computational Applied Mechanics*, 54, pp. 68-86.
- [20] Kumar, B., Joshi, A., Mer, KKS., Prasad, L., Pathak, MK. and Saxena, KK., 2022. The impact of centrifugal casting processing parameters on the wear behaviour of Al alloy/Al2O3 functionally graded materials. *Materials Today: Proceedings*, 62, pp. 2780-6.
- [21] Neves, AMA., Ferreira, AJM., Carrera, E., Cinefra, M., Roque, CMC. and Jorge,

- RMN., 2013. Static, free vibration and buckling analysis of isotropic and sandwich functionally graded plates using a quasi-3D higher-order shear deformation theory and a meshless technique. *Composites Part B: Engineering*, 44, pp. 657–74.
- [22] Rahimi, GH., Arefi, M. and Khoshgoftar, MJ., 2011. Application and analysis of functionally graded piezoelectrical rotating cylinder as mechanical sensor subjected to pressure and thermal loads. *Appl Math Mech-Engl Ed*, 32, pp. 997–1008.
- [23] Arefi, M. and Rahimi, GH., 2014. Application of shear deformation theory for two dimensional electro-elastic analysis of a FGP cylinder. *Smart Structures and Systems*, 13, pp. 1–24.
- [24] Arefi, M. and Rahimi, GH., 2012. Comprehensive thermoelastic analysis of a functionally graded cylinder with different boundary conditions under internal pressure using first order shear deformation theory. *Mechanics*, 18, pp. 5–13.
- [25] Arefi, M. and Zenkour, AM., 2019. Effect of thermo-magneto-electro-mechanical fields on the bending behaviors of a three-layered nanoplate based on sinusoidal shear-deformation plate theory. *Jnl of Sandwich Structures & Materials*, 21, pp. 639–69.
- [26] Ferreira, AJM., Roque, CMC., Neves, AMA., Jorge, RMN., Soares, CMM. and Liew, KM., 2011. Buckling and vibration analysis of isotropic and laminated plates by radial basis functions. *Composites Part B: Engineering*, 42, pp. 592–606.
- [27] Rodrigues, JD., Roque, CMC., Ferreira, AJM., Carrera, E. and Cinefra, M., 2011. Radial basis functions–finite differences collocation and a Unified Formulation for bending, vibration and buckling analysis of laminated plates, according to Murakami’s zig-zag theory. *Composite Structures*, 93, pp. 1613–20.
- [28] Rahimi, GH., Arefi, M. and Khoshgoftar, MJ., 2012. Electro elastic analysis of a pressurized thick-walled functionally graded piezoelectric cylinder using the first order shear deformation theory and energy method. *Mechanics*, 18, pp. 292–300.
- [29] Khoshgoftar, MJ., Rahimi, GH. and Arefi, M., 2013. Exact solution of functionally graded thick cylinder with finite length under longitudinally non-uniform pressure. *Mechanics Research Communications*, 51, pp. 61–6.
- [30] Arefi, M. and Rahimi, GH., 2011. Non linear analysis of a functionally graded square plate with two smart layers as sensor and actuator under normal pressure. *Smart Structures and Systems*, 8, pp. 433–47.
- [31] Ferreira, AJM., Castro, LM., Roque, CMC., Reddy, JN. and Bertoluzza, S., 2011. Buckling analysis of laminated plates by wavelets. *Computers & Structures*, 89, pp. 626–30.
- [32] Chilakala, M., Samyal, R., Garg, S., Saxena, KK. and Gupta, N., 2021. Numerical Simulation of Cracks in Automotive Coatings Under Mechanical and Thermal Loading Using Element Free Galerkin Method. *Advances in Materials and Processing Technologies*, 0, pp. 1–19.
- [33] Kumar, R., Lal, A., Singh, BN., Singh, J., 2022. Numerical simulation of the thermomechanical buckling analysis of bidirectional porous functionally graded plate using collocation meshfree method. *Proceedings of the Institution of Mechanical Engineers, Part L: Journal of Materials: Design and Applications*, 236, pp. 787–807.
- [34] Arefi, M. and Rahimi, GH., 2012. Studying the nonlinear behavior of the functionally graded annular plates with piezoelectric layers as a sensor and actuator under normal pressure. *Smart Structures and Systems*, 9, pp. 127–43.
- [35] Arefi, M. and Rahimi, GH., 2012. Three-dimensional multi-field equations of a functionally graded piezoelectric thick shell with variable thickness, curvature and arbitrary nonhomogeneity. *Acta Mech*, 223, pp. 63–79.
- [36] E. Winkler. Die Lehre von der Elastizitat and Festigkeit. 1867.
- [37] Yaghoobi, H. and Fereidoon, A., 2014. Mechanical and thermal buckling analysis of functionally graded plates resting on elastic foundations: An assessment of a simple refined nth-order shear deformation theory. *Composites Part B: Engineering*, 62, pp. 54–64.

- [38] Thai, H-T., Park, M. and Choi, D-H., 2013. A simple refined theory for bending, buckling, and vibration of thick plates resting on elastic foundation. *International Journal of Mechanical Sciences*, 73, pp. 40–52.
- [39] Malekzadeh, P. and Karami, G., 2008. A mixed differential quadrature and finite element free vibration and buckling analysis of thick beams on two-parameter elastic foundations. *Applied Mathematical Modelling*, 32, pp. 1381–94.
- [40] Sobhy, M., 2013. Buckling and free vibration of exponentially graded sandwich plates resting on elastic foundations under various boundary conditions. *Composite Structures*, 99, pp. 76–87.
- [41] Mognhod Bezzie, Y., Engida Woldemichael, D., 2022. Investigating the graded-index influence on elastic responses of axisymmetric pressurized and heated thick-walled functionally graded material of cylindrical vessel. *Forces in Mechanics*, 7, pp. 100099.
- [42] Mognhod Bezzie, Y., Engida Woldemichael, D., 2021. Effects of graded-index and Poisson's ratio on elastic-solutions of a pressurized functionally graded material thick-walled cylinder. *Forces in Mechanics*, 4, pp. 100032.
- [43] Sayyad, AS., Avhad, PV. and Hadji, L., 2022. On the static deformation and frequency analysis of functionally graded porous circular beams. *Forces in Mechanics*, 7, pp. 100093.
- [44] Vasara, D., Khare, S., Sharma, HK. and Kumar, R., 2022. Free vibration analysis of functionally graded porous circular and annular plates using differential quadrature method. *Forces in Mechanics*, 9, pp. 100126.
- [45] Kumar, R., Lal, A., Singh, BN. and Singh, J., 2020. Non-linear analysis of porous elastically supported FGM plate under various loading. *Composite Structures*, 233, pp. 111721.
- [46] Harsha, A. and Kumar, P., 2022. Thermoelectric elastic analysis of bi-directional three-layer functionally graded porous piezoelectric (FGPP) plate resting on elastic foundation. *Forces in Mechanics*, 8, pp. 100112.
- [47] Kumar, R., Lal, A., Singh, BN. and Singh, J., 2019. New transverse shear deformation theory for bending analysis of FGM plate under patch load. *Composite Structures*, 208, pp. 91–100.
- [48] Ferreira, AJM., Roque, CMC., Jorge, RMN., Fasshauer, GE. and Batra, RC., 2007. Analysis of Functionally Graded Plates by a Robust Meshless Method. *Mechanics of Advanced Materials and Structures*, 14, pp. 577–87.
- [49] Singh, J., Singh, S. and Shukla, KK., 2014. Meshless Analysis of Laminated Composite and Sandwich Plates Subjected to Various Types of Loads. *International Journal for Computational Methods in Engineering Science and Mechanics*, 15, pp. 158–71.
- [50] Solanki, MK., Kumar, R. and Singh, J., 2017. Flexure Analysis of Laminated Plates Using Multiquadratic RBF Based Meshfree Method. *Int J Comput Methods*, pp. 1850049.
- [51] Kumar, R., Bajaj, M., Singh, J. and Shukla, KK., 2022. New HSDT for free vibration analysis of elastically supported porous bidirectional functionally graded sandwich plate using collocation method. *Proceedings of the Institution of Mechanical Engineers, Part C: Journal of Mechanical Engineering Science*, 236, pp. 9109–23.
- [52] Singh, J. and Shukla, KK., 2012. Nonlinear flexural analysis of functionally graded plates under different loadings using RBF based meshless method. *Engineering Analysis with Boundary Elements*, 36, pp. 1819–27.
- [53] Kumar, R., Singh, BN., Singh, J. and Singh, J., 2022. Meshfree approach for flexure analysis of bidirectional porous FG plate subjected to I, L, and T types of transverse loading. *Aerospace Science and Technology*, 129, pp. 107824.
- [54] Kumar, R., Singh, BN. and Singh, J., 2022. Geometrically nonlinear analysis for flexure response of FGM plate under patch load. *Mechanics Based Design of Structures and Machines*, 0, pp. 1–25.
- [55] Kumar, A., Kumar, R., Damania, J. and Singh, J., 2018. Buckling Analysis of FGM Plates by thin plate spline RBF based Meshfree Approach. *IOP Conf Ser: Mater Sci Eng*, 404, pp. 012037.

- [56] Kulkarni, K., Singh, BN. and Maiti, DK., 2015. Analytical solution for bending and buckling analysis of functionally graded plates using inverse trigonometric shear deformation theory. *Composite Structures*, 134, pp. 147–57.
- [57] Sekkal, M., Fahsi, B., Tounsi, A. and Mahmoud, SR., 2017. A new quasi-3D HSDT for buckling and vibration of FG plate, 64, pp. 737–49.